Available online at www.sciencedirect.com
ScienceDirect
International Journal of Mass Spectrometry 267 (2007) 346–356
International Journal of Mass Spectrometry
www.elsevier.com/locate/ijms

A thermal extrapolation method for the effective temperatures and internal energies of activated ions

Michael Meot-Ner (Mautner) [a,b,*], Árpád Somogyi [c,**]

[a] Department of Chemistry, Virginia Commonwealth University, Richmond, VA 23284-2006, United States
[b] Department of Chemistry, University of Canterbury, Christchurch 8001, New Zealand
[c] Department of Chemistry, University of Arizona, Tucson, AZ 85721, United States

Received 28 November 2006; received in revised form 5 April 2007; accepted 5 April 2007
Available online 12 April 2007

In memory of Sharon G. Lias for her contributions to ion chemistry, and for her humaneness.

Abstract

The internal energies of dissociating ions, activated chemically or collisionally, can be estimated using the kinetics of thermal dissociation. The thermal Arrhenius parameters can be combined with the observed dissociation rate of the activated ions using $k_{diss} = A_{thermal}\exp(-E_{a,thermal}/RT_{eff})$. This Arrhenius-type relation yields the effective temperature, T_{eff}, at which the ions would dissociate thermally at the same rate, or yield the same product distributions, as the activated ions. In turn, T_{eff} is used to calculate the internal energy of the ions and the energy deposited by the activation process. The method yields an energy deposition efficiency of 10% for a chemical ionization proton transfer reaction and 8–26% for the surface collisions of various peptide ions. Internal energies of ions activated by chemical ionization or by gas phase collisions, and of ions produced by desorption methods such as fast atom bombardment, can be also evaluated. Thermal extrapolation is especially useful for ion–molecule reaction products and for biological ions, where other methods to evaluate internal energies are laborious or unavailable.

Keywords: Activation energy; Chemical ionization; Collisional activation; Energy transfer; Internal energy

1. Introduction

Activated ions may be formed by various processes such as electron impact (EI), ion–molecule reactions in chemical ionization processes (CI), or collisions with atoms (collision-induced dissociation, CID) or surfaces (surface-induced dissociation, SID). A fraction of the energy of these activating processes can be deposited in the ions as vibrational energy, resulting in fragmentation. For a better understanding of these processes, quantitative information is needed on the energies deposited in the ions.

The internal energies of the ions may be estimated by thermal extrapolation. In this approach, the Arrhenius parameters of thermal dissociation are extrapolated to assign to the activated ions an effective temperature (T_{eff}) at which they would decompose thermally at the same rate, or yield the same products, as the dissociation of the activated ions. This T_{eff} is calculated from $k_{diss} = A\exp(-E_a/RT_{eff})$, where k_{diss} is the observed dissociation rate and A and E_a are the thermal Arrhenius parameters. The T_{eff} calculated by thermal extrapolation can then be used to calculate the internal energies of the ions and the energy deposited by the activating process.

Arrhenius parameters for ion dissociation first became available in the work of Field on protonated esters and ethers [1–4], and for biological ions, on the model dipeptide analogue (*N*-valeryl leucine)H^+ (i.e., $(C_4H_9CONHCH(C_4H_9)COOH))H^+$ ions) [5]. In the latter, we compared thermal dissociation with dissociation following exothermic methane chemical ionization (CI). Extrapolating the thermal Arrhenius parameters for the loss of H_2O, HCOOH (or $H_2O + CO$) or C_4H_9CO to the products of methane CI showed that the product distributions corresponded to temperatures higher by 167 ± 10 K than the gas temperature. This allowed us to introduce effective temperatures (then called

* Corresponding author at: Department of Chemistry, Virginia Commonwealth University, Richmond 23284-2006, USA. Tel.: +804 827 1222; fax: +804 828 8599.
** Corresponding author.
E-mail addresses: mmautner@vcu.edu (M. Meot-Ner (Mautner)), asomogyi@email.arizona.edu (Á. Somogyi).

1387-3806/$ – see front matter © 2007 Elsevier B.V. All rights reserved.
doi:10.1016/j.ijms.2007.04.007

virtual temperatures) as a measure of the energies of activated ions. We also proposed that the high T_{eff} allowed the proton to move endothermically from an amine to a carboxylic group, introducing the mobile proton model of peptide fragmentation [5].

The method of Ref. [5] using thermal Arrhenius parameters to calculate T_{eff} of activated ions may be called "thermal extrapolation" (TEX). The notion of effective (or virtual) ion temperatures (T_{eff}) used in Ref. [5] has been applied subsequently by numerous workers to ions excited by various processes. For example, T_{eff} is often assigned to collisionally activated ions [6–8] and to ions formed in surface-induced dissociation (SID) [9]. These T_{eff} values are derived from CID fragmentation ratios combined with thermochemical or collisional energy information. The physical meaning of T_{eff} has been analyzed theoretically [10–14].

Unlike actual temperatures that are defined thermodynamically, T_{eff} is defined operationally. The meaning of T_{eff} is therefore specific to each application and the relations between effective temperatures derived from various methods are complex. However, in specific cases T_{eff} appears to be meaningful physically. For example, the extended kinetic method that uses T_{eff} often yields gas-phase basicities comparable to equilibrium values. Moreover, Laskin and Futrell [15] showed that collisional activation by CID and SID forms near-Boltzmann distributions, possibly by fast thermalization of translational and internal modes. Therefore, T_{eff} can be meaningful in specific cases, but it is always an approximation whose validity needs to be assessed in each application.

The thermal extrapolation method was applied again in an important advance by Williams and coworkers, who used Arrhenius parameters from Black-Body Infrared Dissociation (BIRD) to calculate T_{eff} for peptide ions [16]. Protonated Leucine enkephalin and doubly protonated Bradykinin ions irradiated in a range of SORI/CID irradiation amplitudes, frequencies and collision gas pressures achieved T_{eff} of 470–670 K for both ions. This new method of thermal extrapolation using BIRD Arrhenius parameters can be productive for large biological ions as the rapid-exchange Arrhenius parameters can be measured readily for large ions in an ICR cell.

Thermal extrapolation from Arrhenius parameters is relatively simple, and it can be applied to complex ions and to the products of ion–molecule reactions for which other methods are not available. The required thermal Arrhenius parameters are increasingly available. Electrospray ionization (ESI) can form ionized biomolecules and the thermal dissociation rates of these ions can be observed by high temperature ion mobility cells [17,18], Turbulent Ion Flow Tube [19] and BIRD [16,20,21].

Thermal dissociation Arrhenius parameters are available for over 220 reactions that will be reviewed elsewhere [22]. However, these data have been used only in a few cases to calculate the energies of activated ions [5,16]. We shall further demonstrate here the use of thermal data and TEX to assign T_{eff} for biological ions, using new data for the amino acid derivative (*N*-valeryl leucine)H^+ activated by various methods, and also for the SID dissociation of peptide ions for which Arrhenius parameters are available. The objective is to assess if TEX gives values that are physically reasonable and trends that are consistent with other estimation methods.

2. Outline of the thermal extrapolation method

The steps of the thermal extrapolation analysis are outlined as follows. The Arrhenius parameters here are the limiting high-pressure, or, in BIRD, the rapid-exchange (REX) limiting *A* factor and the respective activation energies.

2.1. T_{eff} from absolute dissociation rate coefficients

1. The EI, CID or SID spectra and the known dissociation times yield the unimolecular rate constant k_{diss} for reaction (1) of the activated ion M^{+*}, where I_t is the signal intensity of the parent ion and I_o is the sum of parent and fragment ion intensities. For collisional activation, the reaction time *t* is assigned as the time between collision and detection.

$$M^{+*} \rightarrow \text{Fragment}^+ + \text{Neutral} \quad (1)$$

$$I_t = I_o \exp(-k_{diss} t) \quad (2)$$

For chemical activation by exothermic reactions $AH^+ + B$, the dissociating species is the activated BH^{+*} ion, whose dissociation time *t* can be calculated from competition kinetics as described below.

2. The effective temperature T_{eff} is assigned to the rate constant k_{diss} of reaction (1) using Eq. (3) and the thermal Arrhenius E_a and $\log A$ parameters of the same reaction.

$$k_{diss} = A \exp\left(\frac{-E_a}{RT_{eff}}\right) \quad (3)$$

2.2. T_{eff} from relative dissociation rates

Activated ions may dissociate competitively into several channels, and the effective temperature can then be calculated from the branching ratios of these product channels [5,16] using Eq. (4) where *I*, $k_{dissoc,}$ *A* and E_a are the signal intensities, dissociation rate coefficients and Arrhenius parameters of the two dissociation channels, respectively.

$$\frac{I_1}{I_2} = \frac{k_{diss,1}}{k_{diss,2}} = \frac{A_1}{A_2} \exp\left(\frac{E_{a,2} - E_{a,1}}{RT_{eff}}\right) \quad (4)$$

This method is preferable for obtaining T_{eff} as it does not require absolute reaction times that cannot be always estimated reliably. Eq. (4) does not require absolute dissociation rates, but it can be applied only where competitive dissociation channels are observed whose branching ratios are measured and whose absolute or relative Arrhenius parameters are known.

Of course thermal extrapolation can be applied only when the thermal and activated dissociations result in the same fragments. In thermal systems at the high-pressure or rapid-exchange limit, product distribution into any two channels depends only on the HP or REX activation parameters of those channels. Therefore,

thermal extrapolation can be applied for spectra where the two channels appear both in the thermal and activated dissociations.

2.3. Internal energy and energy deposition

3. Using T_{eff} from Eqs. (3) or (4) and the vibrational frequencies of the ions, the Einstein vibrational partition functions yield the internal energies $E_{internal}$ of the ions at temperature T_{eff}, where n_i is the number of oscillators with wave number υ_i and the other symbols have the conventional meanings.

$$E_{internal} = \sum n_i E_{vib,i} = \sum n_i \left(\frac{hc\upsilon_i}{\exp(hc\upsilon_i/kT_{eff})} - 1 \right) \quad (5)$$

4. The internal energies calculated by Eq. (5) result from the original thermal energies of the ions plus the energy deposited by the collisions.

$$E_{internal} = E_{deposited} + E_{thermal} \quad (6)$$

Here $E_{thermal}$ represents the thermal energies of the ions calculated by Eq. (5) at temperature T before activation, and $E_{internal}$ represents the internal energies of the activated ions as calculated by Eq. (5) using T_{eff} from Eqs. (3) or (4). We then obtain $E_{deposited}$ from Eq. (6) and compare it with the chemical or collisional activation energy $E_{activation}$, which is equal to $E_{collision}$ in single-collision CID (center-of-mass collision energy) or SID (laboratory frame energies). For chemical activation, $E_{activation}$ is the exothermicity of the activating reaction, usually proton or charge transfer. Comparing $E_{deposited}$ and $E_{activation}$ yields the chemical to vibrational (C → V) or translational to vibrational (T → V) energy conversion efficiencies.

$$\text{Efficiency}\,(\%) = \frac{E_{deposited}}{E_{activation}} \times 100 \quad (7)$$

As other method for estimating ion internal energies, thermal extrapolation also involves approximations. The activated ions may not have thermal Boltzmann populations, although Laskin and Futrell showed that ions activated by SID and multiple-collision CID can have Boltzmann-like energy distributions [10,15]. Also, the Arrhenius parameters may change with temperature, which affects the application of Arrhenius parameters measured at one temperature to dissociation at another, usually higher, effective temperature. Further, the populations of the activated ions do not become re-thermalized after part of the ion population dissociates, as they would in thermal dissociation. Some of the ions may dissociate rapidly before detection or deactivation, while other ions may have too little energy to dissociate even at longer times [23–25]. For these reasons, the ions may not decompose exponentially as assumed in Eq. (2) and the assigned k_{diss} may not be accurate. The effects of these factors on the calculated T_{eff} and $E_{internal}$ need to be investigated.

3. Computational and experimental methods

The preceding section outlined the main steps of the thermal extrapolation method. Details of the computations relevant to the present systems, and experimental methods, are described in this section.

3.1. Computational methods

In Eq. (2), the value of I_t/I_o represents the fraction of the remaining parent ion (MH^+) after dissociation time t, calculated from Eq. (8).

$$\frac{I_t(MH^+)}{I_o(MH^+)} = \frac{I(MH^+)}{I(MH^+) + \sum \Delta I(\text{Fragments})} \quad (8)$$

In SID studies, the ratio of the intensity of the fragments to the total ion intensity, I_t/I_o is plotted as a function of laboratory collision energy. This function is called the fragmentation efficiency curve. SID fragmentation efficiency curves have been used to reveal the relative energetics of peptide fragmentation as a function of peptide sequence and amino acid composition [26–29]. The dissociation time from the surface impact to detection in our instrument was calculated as 6.2 μs for (Leucine enkephalin)H^+ based on instrument tuning and geometry parameters [30]. For other protonated peptides in our studies, the calculated dissociation times were: Leucine enkephalin dimer, 8.8 μs; $Glycine_5$, 4.6 μs; $Glycine_5$ Dimer, 6.5 μs, and des-Arg^9 Bradykinin, 7.9 μs. These values are based on the assumption that all the ions leave the surface with the same kinetic energy so that their velocity ratios can be calculated as the square root of the inverse mass ratios.

Arrhenius parameters for use in Eqs. (3) and (4) are obtained from thermal dissociation studies. The fragmentation and Arrhenius parameters for (*N*-valeryl leucine)H^+ are described below. The parameters for des-Arg^9 Bradykinin and (Leucine enkephalin)H^+ in Table 1 are cited from our experiments that used thermal dissociation in the heated electrospray capillary [30] or from BIRD studies of Williams and co-workers [31,32], which are supported by ion trap measurements [33,34]. All these methods yield only approximate high-pressure or rapid-exchange limiting Arrhenius parameters. The results from the heated capillary and BIRD measurements are different, but the E_a and $\log A$ values obtained by the two experiments differ in a manner that the yields $E_{deposited}$ values consistent within about a factor of two.

Calculating internal energies in Section 2.3 requires the vibrational frequencies of the ions. For peptide ions, the frequencies may be calculated by ab initio methods or approximated by group frequencies (see Appendix A). As a test, we assigned the frequencies of the various structural groups of (Leucine enkephalin)H^+ to calculate $E_{internal}$ as a function of temperature. Subsequently, we also used ab initio frequencies[1] to calculate $E_{internal}$ on this basis. Fig. 1 shows that $E_{internal}$ calculated using either set of frequencies is similar, and the calculated E_{dep} and %efficiency are therefore also similar. Estimated group frequencies are useful for biological ions where experimental or ab initio vibrational frequencies are not available.

[1] C. Bleiholder, B. Paizs, personal communication, 2005.

Table 1
Mass spectra of (*N*-valeryl leucine)H^+ obtained on various instruments

	Ion					
	MH^+ (*m/z* 216)	MH^+–H_2O (198)	MH^+–H_2O–CO (170)	MH^+–C_4H_8O (132)	MH^+–C_4H_8O–HCOOH (86)	Primary product distribution (132 + 86)/(198 + 170)
Methane CI						
390 K[a]		47.8	34.0	18.2		1.1
460 K[a]		43.5	19.8	36.7		1.3
SORI/CID						
0.2 V	52.2	4.8	6.7	22.8	13.5	3.2
0.5 V	9.3	4.5	7.7	33.1	45.1	6.4
1.0 V	0.0	2.0	4.4	24.5	69.1	14.6
Ion Trap						
16% *E*	92.6	4.6	0.0	2.8	0.0	0.6
30% *E*	0.0	48.3	12.1	37.7	1.9	0.7
FAB/metastables	86.8	3.9	2.4	6.8	0.1	1.1
FAB/10 keV CID[b]	67.0	5.4	4.7	18.9	4.0[c]	2.3

Normalized ion intensities $100I_i/\sum I$. Data from present work unless otherwise noted.
[a] From data of Ref. [5]. Intensities of MH^+ parent ion were not given, however the relative normalized intensities of the listed ions can be used for calculating T_{eff} from competitive dissociation kinetics.
[b] The center of mass energy (maximum available energy) is 1562 eV for a single collision with Ar.
[c] Both *m/z* 85 and 86 appear in the spectrum, 86 indicates their sum.

To calculate the energy deposited by the collisions, we must subtract from $E_{internal}$ the thermal energy that the ions contained before activation. In our SID experiments [30] the ions were generated by ESI using a heated capillary at 425 K and we use Eq. (5) and the group frequencies in Appendix A to calculate the thermal energy at this temperature. Table 2 shows that the thermal energy can be significant for large ions with many internal modes.

3.2. Experimental methods

N-valeryl leucine was synthesized by a condensation reaction of valeric acid and leucine. MS and MS/MS experiments were carried out on a Thermoelecton (Finnigan) LCQ Classic Ion Trap instrument by using electrospray ionization (ESI). *N*-valeryl leucine was dissolved in MeOH:H_2O 1:1 in a concentration range of 50–80 μmol and was sprayed with conventional ESI conditions. Helium (He) was used as a collision gas with a conventional pressure in the ion trap. Relative excitation energies of 15–30% were used.

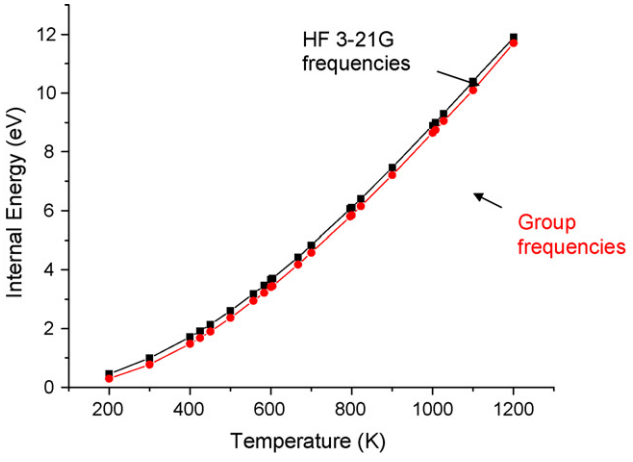

Fig. 1. Internal energies of (Leucine enkephalin)H^+ ions as a function of temperature, calculated using ab intio HF3-21G (top line) and estimated group frequencies (bottom line).

The FAB metastable dissociation mass spectra of (*N*-valeryl leucine)H^+ were obtained on a JEOL HX110A EB mass spectrometer with a FAB Xe gun. The matrix of 50% glycerol, 25% thioglycerol, and 25% *m*-nitrobenzyl alcohol (containing 0.1% of TFA) was used. High energy (10 keV) CID has also been applied for (*N*-valeryl leucine)H^+ ions generated by FAB with a collision gas of Ar, where more fragments were observed relative to the surviving (*N*-valeryl leucine)H^+ ion and the ratio of *m/z* 132/198 increased from ca. 1.8 to 3.5 upon keV CID. The ions at *m/z* 86 and 85 also appeared in the 10 keV CID spectra although with low intensity and $I(85)$:$I(86) \approx 0.5$. These spectra show that the internal energies of the selected (*N*-valeryl leucine)H^+ ions are higher in 10 keV CID than in the metastable spectrum, although significant amount of internal energy is already deposited by FAB ionization itself.

Sustained off-resonance irradiation (SORI)-CID experiments were carried out on an IonSpec 4.7 T Fourier transform ion–cyclotron resonance (FT-ICR) instrument. Argon (Ar) was used as a collision gas with a pressure pulse of 2×10^{-7} Torr. SORI excitation voltages were varied in the range of 0.1–1.0 V. The SORI excitation time was 500 ms in each experiment. The MH^+ ions were formed by a second generation Analytica ESI source under normal operating conditions (e.g., needle voltage 3.8 kV, capillary temperature 60 °C, capillary voltage 80 V).

The details for SID experiments have been published in Refs. [27,30]. An octadecanethiol (C18) surface prepared on vapor deposited gold was used in the present study. The laboratory collision energy was varied by changing the potential difference between the ion source and the surface (multiplied by the appropriate charge state).

Table 2
Effective temperatures of (*N*-valeryl leucine)H^+ ions calculated by thermal extrapolation, and internal energies and energy deposition by chemical ionization, gas-phase collisions, and FAB ionization

Activation method	Activation process	T_{eff}[a]	$E_{activation}$[b]	E_{int}[b]	$E_{thermal}$[b]	E_{dep}[b]	%Efficiency
Chemical ionization	CI (proton transfer from CH_5^+ at 390 K)	492[c]	4.08[d]	1.05[e]	0.68[f]	0.37[g]	9.0[h]
	CI (proton transfer from CH_5^+ at 460 K)	567[c]	4.08[d]	1.37[e]	0.93[f]	0.45[g]	11.1[h]
Gas collisions	CID SORI 0.2 V	776[i]	(0.2 V)[j]	2.44[k]	0.41[f]	2.03[g]	(10.2)[l]
	CID SORI 0.5 V	918[i]	(0.5 V)[j]	3.28[k]	0.41[f]	2.87[g]	(5.7)[l]
	CID SORI 1.0 V	1164[i]	(1.0 V)[j]	4.90[k]	0.41[f]	4.48[g]	(4.5)[l]
Gas collisions (ion trap)	CID (He, ion trap, 300 K)	592[i]	(16%)[j]	1.49[k]	0.41[f]	1.08[g]	
		596[i]	(30%)[j]	1.51[k]	0.41[f]	1.10[g]	
FAB/metastable		631		1.68[k]	0.41[m]	1.27	
FAB/10 keV CID		724		2.16[k]	0.41[m]	1.75	

[a] In Kelvin.
[b] In eV.
[c] Values of T_{eff} recalculated from data of Ref. [5] assuming *m/z* 198 → 170 and *m/z* 130 → 86 consecutive dissociation (see text).
[d] Activation by proton transfer from CH_5^+ in methane with estimated exothermicity of 94 kcal/mol. (PA(CH_4) = 129.9 kcal/mol, PA(*N*-valeryl leucine) = 224 kcal/mol, estimated on basis of amides.
[e] Ion internal energies calculated from T_{eff} using ab initio frequencies.
[f] Thermal energies of the ions (eV) from heated capillary or ion source temperatures, calculated using capillary or ion trap temperature, ab intio frequencies and Einstein functions.
[g] Energies deposited in the ions by exothermic proton transfer or ion trap collisions, using $E_{internal} = E_{deposited} + E_{thermal}$.
[h] Efficiency of energy deposition, efficiency = (E_{dep}/E_{coll}) × 100.
[i] T_{eff} calculated using product distributions (Table 1), adding the *m/z* 198 + 170 and 132 + 86 intensities to account for primary dissociation channels. Arrhenius parameters for competitive dissociation were obtained from data of Ref. [5] with slight correction considering HCOOH loss as consecutive $H_2O + CO$ loss. For H_2O loss this correction gave log A = 9.7, Ea = 15.0 kcal/mol compared with log $A = 9.7 \pm 1.0$, $E_a = 15.2 \pm 1.5$ kcal/mol in Ref. [5]. For C_4H_8O loss, the corrected parameters were log $A = 12.2$, $E_a = 22.1$ kcal/mol compared with log $A = 12.1 \pm 1.0$, $E_a = 22.1 \pm 1.5$ kcal/mol in Ref. [5].
[j] Nominal LCQ Ion Trap or SORI energies. Ion trap collision gas He at 300 K; SORI collision gas Ar at 300 K.
[k] Ion internal energies calculated using ab initio frequencies.
[l] Nominal efficiencies calculated from $E_{deposited}/V$ where V is the nominal SORI collision energy.
[m] Calculated from FAB metastable dissociation mass spectra obtained in a Magnetic Sector/TOF Mass Spectrometer. Energies were calculated from FAB metastable dissociations spectra (Table 1), $E_{thermal}$ corresponds to the neutral at 300 K. Ion internal energies calculated using ab initio frequencies.

4. Results

4.1. Mass spectra of (N-valeryl leucine)H^+

Activation of (*N*-valeryl leucine)H^+ ($C_4H_9CONHCH(C_4H_9)COOH)H^+$ by various processes was examined using chemical ionization data from Ref. [5], and new Ion Trap, SORI-CID and FAB activation experiments from this work. This ion was selected because it is a simple dipeptide analogue whose high-pressure limiting Arrhenius activation parameters are available [5].

The mass spectra in Table 1 and Ion Trap MS/MS spectra showed that the (MH^+) ion (*m/z* 216) undergoes primary dissociation with the loss of H_2O to yield a b-type ion (*m/z* 198) followed by loss of CO (*m/z* 170), or alternative primary dissociation with the loss of C_4H_8CO (*m/z* 132) to yield a y-type ion followed by loss of HCOOH (*m/z* 86). This mechanism as shown in Scheme 1 is consistent with ab initio calculations.[1] Accord-

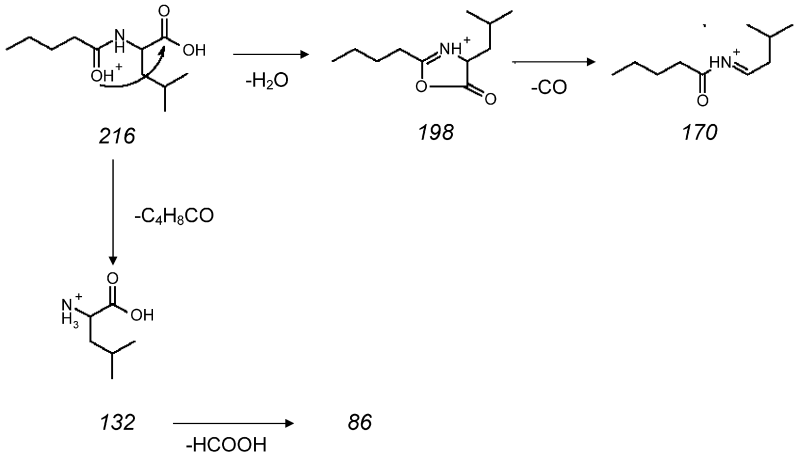

Scheme 1.

ingly, to calculate T_{eff} we added the intensities of (198 + 170) and (132 + 86) to account for product distributions into the primary channels. For the *m/z* 198 primary channel we used $\log A = 9.7$ and $E_a = 15.0$ kcal/mol and for the *m/z* 132 primary channel we used $\log A = 12.2$ and $E_a = 22.1$ kcal/mol. These Arrhenius parameters from Ref. [5] were re-calculated using the original data but the mechanism of Scheme 1 rather than the one-step loss of HCOOH from the molecular ion in Ref. [5] (see Table 2, footnote i).

Table 1 shows the mass spectra obtained by various methods. Consistent with the relative E_a values, increasingly energetic activation increases the higher energy (*m/z* 132 + *m/z* 86) ions compared with the (*m/z* 198 + *m/z* 170) ions. Consistent with the consecutive mechanism, increasingly energetic collisional activation also increases the secondary/primary ion ratios in each channel.

4.2. Energy deposition by exothermic reactions: Chemical ionization

Energy deposition by exothermic reactions converts chemical energy to vibrational energy (C → V conversion). In chemical ionization, we consider the total activation energy as the exothermicity of a proton transfer reaction. We recalculated T_{eff} of the chemically activated (*N*-valeryl leucine)H^+ ions the data in Table 1 and Eq. (4) using the mechanism of Scheme 1 as described in the preceding section. For the CI experiments at four gas temperatures we found (T_{source} and respective recalculated T_{eff}) of 390 and 492; 410 and 543; 447 and 576; 460 and 567 K. The derived T_{eff} is higher by an average 118 ± 16 K than the actual gas temperatures, due to excitation by the exothermic protonation reaction.

Using these T_{eff} values and Eqs. (5)–(7) we can calculate the internal energies of the ions and the energy deposition by the proton transfer reaction. We use Eq. (5) to calculate $E_{thermal}$ at the actual gas temperatures in the ion source and $E_{internal}$ of the ions after chemical ionization. The difference yields $E_{deposited} = 0.37$ and 0.45 eV (8.5 and 10.4 kcal/mol) by protonation at $T_{source} = 390$ and 460 K, respectively. Compared with the exothermicity of 94 kcal/mol for proton transfer from CH_5^+ to *N*-valeryl leucine, 9.0% or 11.1% of the exothermicity is deposited as internal energy of the ions, respectively, with the energy deposition efficiency changing little in this temperature range. We note that the $C_2H_5^+$ ion in methane CI can also protonate *N*-valeryl leucine with an exothermicity of 61 kcal/mol, but protonation by CH_5^+ is more exothermic and we assume that most of the observed fragmentation occurs from this protonation reaction.

These calculations used branching ratios into competitive channels, which is the preferred method when available as noted above. However, T_{eff} can be assigned under high-pressure CI conditions from one dissociation channel, using competitive fragmentation and collisional stabilization.

$$\begin{aligned} &AH + B \xrightarrow{k_{coll}} BH^{+*} \\ &BH^{+*} \xrightarrow{k_{uni}} F^+ \end{aligned} \qquad (9)$$

$$\begin{aligned} &BH^{+*} \xrightarrow{k_s[M]} BH^+ \\ &\frac{F^+}{BH^+} = \frac{k_{uni}}{k_s[M]} \end{aligned} \qquad (10)$$

Here k_{uni} is the rate constant for the dissociation of the activated BH^{+*} ions to form fragment ion F^+ and k_s is the rate constant for stabilization by third-body M. For efficient polyatomic third-body gases k_s may be equated with the collision rate coefficient $k_{coll(BH^+,M)}$ that can be calculated by Langevin or ADO theory [35]. Eq. (10) can then yield the dissociation rate k_{uni} of the excited BH^{+*} ions formed by the exothermic reactions, and T_{eff} and the energy terms can be calculated from k_{uni} as above.

An inverse of the thermal extrapolation method can be used to calculate the efficiency of collision stabilization of activated ions. The internal energies of the ions may be known or assumed, for example, by equating them with the exothermicity, and k_{uni} (and the Arrhenius parameters) may be calculated by Master Equation modeling. Combining k_{uni} with the observed product ratio F^+/BH^+ in Eq. (10) yields the stabilization rate constant k_s which can be used to calculate $k_s/k_{coll(BH^+,M)}$ representing the efficiency of third-body stabilization of BH^{+*} by [M]. This method was used by Troe et al. for stabilization of activated ethylbenzene ions in the $O_2^+ + He$ or N_2 systems [36].

4.3. Energy deposition by surface collisions and FAB desorption

Table 3 shows data for dissociation following surface collisions, and the energy terms calculated for various peptide ions. For (Leucine enkephalin)H^+ the T_{eff} was calculated using Arrhenius parameters from thermal capillary [30] and BIRD studies [31,32]. The energy terms were calculated using ab initio frequencies[1] or group frequencies, with similar results.

Table 3 shows results at different SID collision energies for five different peptide ions. For all of the ions, the calculated $E_{deposited}$ is approximately proportional to $E_{collision}$ and consequently the T → V conversion efficiencies defined as $(E_{deposited}/E_{collsion}) \times 100$ vary little with SID collision energy. The increasing T_{eff} and $E_{deposited}$ with increasing $E_{collision}$ is similar to the results of (*N*-valeryl leucine)H^+ in Table 2 under SORI-CID.

Table 3 includes the CID dissociation of the (Leucine enkephalin)$_2H^+$ dimer. The calculations show that it absorbs more of the collision energy than the monomer ion, possibly due to efficient energy deposition into the low-frequency noncovalent intermolecular bonds. This mechanism needs further study as the $(Gly_5)_2$ H^+ dimer does not show this effect.

Considering the various approximations of the thermal extrapolation method, it is encouraging that the calculated energy deposition efficiencies for the various ions by SID are consistently 10–25%, which is only slightly higher than the range found for alkanethiolate surfaces by other energy estimation methods. Note, however, that all other methods use approximations and were applied for smaller projectiles (see further discussion below).

Table 3
Effective temperatures, internal energies and energy deposition calculated by thermal extrapolation for peptide ions activated by surface collisions with an octadecanethiolate surface on gold

Dissociating ions, and neutrals loss	Activation method	Source of E_a and log A	I/I_o	log k[a]	E_a[b]	log A[b]	T_{eff}[c]	E_{coll}[d]	E_{int}[e]	$E_{thermal}$[f]	E_{dep}[g]	%Effici-ency[h]
Surface collisions (SID)												
Leu enkephalin $(YGGFL)H^+$ to fragments	Low E SID	Heated capillary[i]	0.8	4.56	1.67	15.7	754	23.0	5.25 (5.51)	1.68 (1.92)	3.57 (3.59)	15.5 (15.7)
	Medium E SID	Heated capillary[i]	0.5	5.05	1.67	15.7	789	27.6	5.70 (5.96)	1.68 (1.92)	4.02 (4.04)	14.6 (14.6)
	High E SID	Heated capillary[i]	0.2	5.41	1.67	15.7	817	31.9	6.07 (6.33)	1.68 (1.92)	4.39 (4.41)	13.8 (13.8)
	Low E SID	BIRD[j]	0.8	4.56	1.09	10.5	926	23.0	7.58 (7.84)	1.68 (1.92)	5.90 (5.92)	25.6 (25.8)
	Medium E SID	BIRD[j]	0.5	5.05	1.09	10.5	1010	27.6	8.80 (9.05)	1.68 (1.92)	7.12 (7.13)	25.8 (25.9)
	High E SID	BIRD[j]	0.2	5.41	1.09	10.5	1082	31.9	9.87 (10.1)	1.68 (1.92)	8.19 (8.18)	25.7 (25.6)
Leu enkephalin dimer $(YGGFL)_2H^+$ to $(YGGFL)H^+$	SID	Heated capillary[i]	0.5	4.89	2.02	21.7	607	13.8	7.02	3.39	3.63	26.4
	SID	BIRD[j]	0.5	4.89	1.60	17.2	657	13.8	8.18	3.39	4.79	34.7
$(Glycine)_5H^+$ to fragments	Low E SID	Heated capillary[k]	1.25	4.69	0.86	10.7	726	19.0	2.55	0.92	1.63	8.6
	Medium E SID	Heated capillary[k]	2.00	5.18	0.86	10.7	790	24.3	2.96	0.92	2.04	8.4
	High E SID	Heated capillary[k]	5.00	5.54	0.86	10.7	846	28.6	3.34	0.92	2.42	8.5
$(Glycine_5)_2H^+$ to $(Glycine)H^+$	Low E SID	Heated capillary[k]	1.25	4.54	2.20	24.7	552	11.4	3.07	1.83	1.24	10.9
	Medium E SID	Heated capillary[k]	2.00	5.03	2.20	24.7	565	15.5	3.21	1.83	1.38	8.9
	High E SID	Heated capillary[k]	5.00	5.40	2.20	24.7	576	19.0	3.34	1.83	1.51	8.0
(Des-Arg^9 Bradykinin)H^+ to fragments	Low E SID	BIRD[l]	1.25	4.45	1.20	12.0	805	66.8	9.8	2.8	7.0	10.5
	Medium E SID	BIRD[l]	2.00	4.94	1.20	12.0	861	77.5	11.1	2.79	8.31	10.7
	High E SID	BIRD[l]	5.00	5.31	1.20	12.0	908	87.0	12.1	2.8	9.3	10.7

[a] SID dissociation rate constant (s^{-1}) from Eq. (1).
[b] E_a (eV) and log A values from the references in footnotes i, j, k and l.
[c] Effective temperature (K) of activated ions from Eq. (2).
[d] SID collision energies (eV).
[e] $E_{internal}$ energy of decomposing ions calculated using T_{eff}, by using estimated group frequencies (see Appendix A) and ab initio (3BLYP) frequencies (in parenthesis).
[f] Thermal energies of the ions (eV) from the heated electrospray capillary, calculated using estimated group frequencies and Einstein functions.
[g] Energies deposited in the ions by SID collisions, using $E_{internal} = E_{deposited} + E_{thermal}$.
[h] Efficiency of energy deposition, efficiency $= (E_{dep}/E_{coll}) \times 100$.
[i] Ref. [30].
[j] Ref. [32].
[k] From thermal decomposition in heated electrospray capillary (Meot-Ner et al., unpublished results).
[l] Ref. [31].

An interesting application is for the energies of ions produced by FAB. For example, Table 2 shows that the dissociation product distributions of (*N*-valeryl leucine)H^+ ions produced by FAB and undergoing metastable dissociation corresponds to 631 K, and activation by collisions with Ar atoms increases this to 724 K. Since competitive kinetics were used for calculating T_{eff}, these results reflect only the energies of the dissociating ions, whether or not most of ions produced by FAB dissociate. The high calculated T_{eff} values are consistent with the tendency of FAB to generate high-energy ions. Similarly, T_{eff} can be calculated for ions produced by other desorption methods such as MALDI.

4.4. T_{eff} and internal energies in gas-phase collisions: SORI-CID

We examined the SORI-CID dissociation of (*N*-valeryl leucine)H^+ ions. The mass spectra in Table 1 show primary product distributions and enhanced secondary dissociation compared with other methods that suggest high energies of the dissociating ions. These parameters also increase with increasing SORI voltage and collision energy as expected. Correspondingly, the T_{eff} and $E_{internal}$ calculated from the product branching ratios for these ions in Table 2 are high, and they increase with increasing collision energy.

As for the energy deposition efficiencies, they cannot be calculated because multiple collisions occur in SORI-CID and the collision energies are not well defined. However, the maximum kinetic energy and maximum center-of-mass collision energy can be calculated in SORI-CID processes so that a lower limit for energy conversion can be estimated. This approach will be elaborated in a subsequent paper on protonated *N*-valeryl leucine.

As noted above, thermal extrapolation was applied to SORI-CID fragmentation by Williams and coworkers to calculate T_{eff} using Arrhenius parameters from BIRD [16,31,32]. (Leucine enkephalin)H^+ and (Bradykinin)$_2H^{2+}$ ions were irradiated in a range of amplitudes and frequencies and collision gas pressures achieved T_{eff} of 470–670 K. Both absolute dissociation rates and relative rates of b_4 ion/H_2O loss gave similar T_{eff} for (Leucine enkephalin)H^+ suggesting that this ion can be a useful ion thermometer [32]. The use of Arrhenius parameters from BIRD to calculate T_{eff} is a significant new approach that is particularly suitable for biological ions, as rapid-exchange Arrhenius parameters for large ions can be measured readily by BIRD methods.

4.5. T_{eff} and internal energies in ion traps

Table 1 shows the CID mass spectra of (*N*-valeryl leucine)H^+ in collisions with He atoms in an ion trap instrument. Table 2 shows T_{eff} and energy deposited in ions calculated from dissociation branching ratios by thermal extrapolation. The log *A* and E_a parameters used in the calculations were again from Ref. [5] with the small adjustments noted above.

Table 1 shows results at two extreme energies, at "16% energy" where the fragment ions just appear, and at "30% energy" where total fragmentation is observed. The primary product distributions in Table 1 indicate dissociation from lower energy populations, and correspondingly Table 2 indicates lower T_{eff} of the dissociating ions in the ion trap at both nominal collision energies compared with other methods.

Although the amount of fragmentation increased significantly from "16% energy" to "30% energy", the ratios of the primary product channels remained effectively constant, despite their different Arrhenius parameters. Correspondingly, the T_{eff} calculated from the product ratios remains constant at 595 ± 10 K over this range. This is some 300 K higher than the gas temperature, due to energy deposition of about 1.5 eV (35 kcal/mol) by the collisions at both nominal collision energies. The observation that the ion energies and T_{eff} do not change with collision energy is different from the trends observed in the other methods.

These results may be due to multiple collisions in the ion trap. The energy deposition efficiencies also cannot be evaluated because the collision energies are not well defined. However, the observed product ratios and the TEX analysis are still useful to indicate that ions dissociate in ion traps from lower-energy states than in other methods.

5. Discussion

5.1. Sensitivity to experimental and calculated parameters

As noted above, calculating T_{eff} from relative dissociation rates into competitive channels is preferable to the use of absolute rate coefficients. In fact, using relative product distributions may be the only possible TEX method when very small or large extents of fragmentation occur and the ratios of the precursor ion to fragment ions are beyond the dynamic range of the mass spectrometer. In these cases I_t/I_o and therefore k_{diss} cannot be determined, but relative product ratios can be still measured accurately.

Of course, the dynamic range also limits the measurable T_{eff} even using competitive channels. For example, assume that the primary fragment ions MH^+–H_2O and MH^+–C_4H_8CO in the dissociation of (*N*-valeryl leucine)H^+ have branching ratios of 100:1 or 1:100, which is usually the limit of accurate measurement. With these ratios, the Arrhenius parameters (Table 2, footnote i) would give $T_{eff} = 345$ or 3103 K, respectively, and T_{eff} outside this range could not be measured.

The uncertainties of the Arrhenius parameters can affect the TEX results. For example, Table 3 shows T_{eff} and $E_{internal}$ calculated for the SID fragmentation of(Leucine enkephalin)H^+ using two sets of Arrhenius parameters. Although the log *A* and E_a values vary significantly, they vary in a compensating manner between the two sets, and as a result the calculated $E_{internal}$ and $E_{deposited}$ and the deposition efficiency varies less extensively than they would by either factor alone.

To analyze these effects, we considered (Leucine enkephalin)H^+ ions that decompose with a rate constant of $\log k_{diss} = 5.05$, corresponding to SID at medium energy. We calculated the internal energies of these ions by TEX using a range of Arrhenius parameters. Fig. 2 shows the

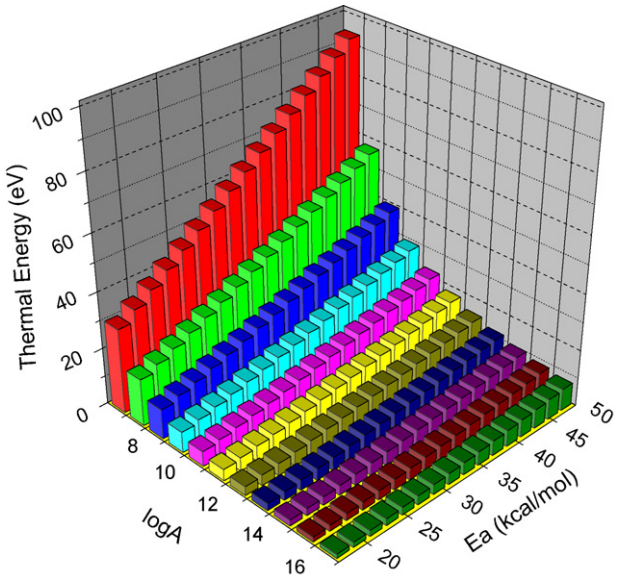

Fig. 2. The calculated internal energy by thermal extrapolation (in eV) for the dissociation of (Leucine enkephalin)H^+ at the rate of $\log k = 5.05\ s^{-1}$, corresponding to SID at medium surface collision energy. The figure shows the calculated internal energy as a function of the Arrhenius A factor and activation energy (E_a, kcal/mol) that are used in thermal extrapolation calculations.

internal energy calculated using $\log A$ factors range of 7–17 and E_a values between 18 and 50 kcal/mol. For more common values of $\log A = 11$–17 and $E_a = 20$–35 kcal/mol the calculated energies of 1–10 eV are relatively insensitive to the Arrhenius parameters and their uncertainties. This internal energy is commonly achieved in many tandem MS/MS instruments. However, for reactions with low $\log A$ (<10) and high E_a (>40 kcal/mol) values the calculated energy is sensitive to the Arrhenius parameters and their uncertainties.

Calculating $E_{internal}$ requires vibrational frequencies that may be available only as estimated groups of frequencies, especially for large ions. We can compare the use of group versus ab initio frequencies for (Leucine enkephlin)H^+ ions[1] using the estimated group frequencies as shown in Appendix A. The estimations were based on the structures of the ions, for example, the 1650 cm^{-1} group frequency can be attributed to the amide-I band wavenumber. Similarly, the frequency group of 3000 cm^{-1} can be set by the number of C–H bonds. Generally, group frequencies slightly underestimate some lower energy vibrations. This is manifested in slightly lower thermal energies obtained by the group frequencies than by the calculated frequencies as shown in Fig. 1. A new estimation method for the vibrational frequencies of amino acid residues [37] may eliminate the need to use group frequencies for peptide ions. Nevertheless, Fig. 1 and also Table 3 show that the ab initio and group frequencies yield comparable results.

5.2. *Thermal extrapolation for ion thermometry, and comparison with other methods*

Thermal extrapolation can serve as ion thermometry in that it assigns effective temperatures to activated ions, bearing in mind that the calculated values are approximations for non-thermal ion populations. Ideally, an ion thermometer molecule in this method should have a simple dissociation pattern with two competitive channels that have accurately measured high-pressure or REX Arrhenius parameters. It is desirable that there will be large differences between the activation energies of the two channels, which make the product ratios sensitive to the internal energies. This increases the sensitivity and resolution of the TEX calculations but it also increases the uncertainty of the calculated T_{eff} values.

Several methods have been applied for ion thermometry to estimate the internal energies of collisionally activated ions and the energy deposition efficiencies, as reviewed recently by Laskin and Futrell [10,15]. A main method deconvolutes the fragmentation graphs of thermometer molecules, usually from photoelectron–photoion coincidence (PEPICO) measurements, and compares these with fragmentation following CID or SID activation to assign the internal energies of the collisionally activated ions. Ferrocene and metal carbonyl ions that lose (CO) ligands stepwise were applied as thermometer molecules [9,38–41]. The drawbacks are that not many breakdown graphs are available, and the breakdown graphs are affected by instrument-dependent kinetic shifts. In comparison, limiting high-pressure or REX thermal Arrhenius parameters are intrinsic to the ions and independent of instruments.

Values of $E_{internal}$ were also deduced from crossed molecular beam experiments where ions prepared with well-defined distributions of internal energies are collided with a beam of neutral atoms. The kinetic energies, identities, and scattering angles of product ions are measured and momentum conservation laws are followed by integration over scattering angles gives the collisional energy deposition function [10,42–46]. Theoretical simulations of the collisions [47–51] and comparing the observed fragmentation with theoretical predictions based on ab initio energies and statistical factors of the transition states, combined with unimolecular RRKM calculations, were also applied [52,53]. Other specific examples include internal energy estimations for the ions of benzene [54,55] bromobenzene [56], butylbenzene [57], and small peptides [10,15,24,25,58–61].

In some cases T_{eff} rather than $E_{internal}$ was assigned to the ions. For example, Williams and coworkers assigned T_{eff} of 470–670 K to (Leucine enkephalin)H^+ [32] and (Bradykinin)$2H^{2+}$ ions [31]. Laskin and Futrell assigned T_{eff} of 2000 K to the $C_6H_6Br^{\bullet+}$ and $C_{10}H_7Br^{\bullet+}$ ions [56] and 472–1390 K for the dialanineH^+ (AAH^+), depending on the number and energy of collisions, for ions produced by SORI at various collision numbers and energies [58]. In her more recent work, Laskin calculated the energetics and dynamics for seven SID fragmentation channels of protonated Leucine enkephalin [61]. This work also discussed the variation of the Arrhenius parameters with temperature, which can affect the application of thermal extrapolation.

Trends that emerged from these methods are that:

- The SID energy deposition efficiencies are comparable for impacting ions of a wide range of sizes and structures. In general, T → V conversion values are reported for small

projectile ions in the range of 10–19% on hydrocarbon surfaces [15,25,54,62]. On fluorinated hydrocarbon surfaces, the T → V efficiencies are characteristically higher (15–25%).
- The deposited energy increases with collision energy, and consequently, the deposition efficiencies vary only weakly over a wide range of collision energies.

The results of the thermal extrapolation method in Table 3 agree with the general trends. The efficiencies for T → V conversion for (Leucine enkephalin)H^+ from thermal extrapolation are 13.8–15.5% using the heated capillary Arrhenius parameters, and 25.6–25.8% using the BIRD parameters. The latter values are higher than those reported for alkanethiolate surfaces. On the other hand, our results for des-Arg^9 bradykinin (10.7%) using BIRD parameters agree well with the value published by Laskin et al. (10.1%) [25]. With relation to these SID spectra, Laskin et al. found that they are affected significantly by kinetic shifts [23]. Furthermore, it needs to be established if the Arrhenius parameters from BIRD studies that we used for the analysis are truly REX parameters for these small peptides.

The observed general trend is that a similar fraction of collisional energy is deposited in ions for a wide range of ions and collisions. Energy deposition in the ion results from distribution of the kinetic energy into the translational energy of recoil, the thermal energy of the surface and the internal energy of the ion. Energy deposition is complex, but as a matter of interest, simple equipartition among these modes would result in a constant 1/3T → V conversion efficiency regardless of the collision energy. The independence on collsion energy is consistent with the observed trends although the observed conversion efficiencies are smaller than the 1/3 equpartition ratio. This suggests that the collisions deposit more energy into the recoil translational energy than into the internal energy. Of course, energy partitioning is complex and requires more detailed analysis such as, for example, the dynamic simulations by Hase and coworkers [47–51].

6. Conclusions

Thermal extrapolation of Arrhenius parameters can be used to evaluate T_{eff} and the energies of chemically or collisionally activated ions. The results assign T_{eff} at which thermal dissociation would occur at the same rate, or lead to the same product distributions, as the observed activated fragmentation pathways.

The T_{eff} values can be assigned based on absolute dissociation rates or based on relative dissociation rates into competitive channels. The latter is particularly useful when absolute k_{diss} cannot be assigned because the reaction time is uncertain or because very small or large extents of fragmentation occur.

Thermal extrapolation and other methods of energy estimates assign T_{eff} values to activated ions. Although the ions have non-thermal populations, the internal energy distributions produced by CID or SID can closely approximate thermal distributions [10,15]. Consequently, the assigned T_{eff} vales may be physically meaningful.

In the present examples we applied thermal extrapolation to various biological ions for whose dissociation both Arrhenius parameters and activated dissociation data are available. The resulting energy deposition efficiencies are mostly in the range of 8–25% and they are consistent with estimates by other methods. The trend of nearly constant deposition efficiency calculated by TEX over a range of collision energies is also consistent with other observations.

Thermal extrapolation offers a simple way to estimate the energies of ions activated by various methods including CI, CID or SID and internal energies deposited by soft ionization methods such as ESI, FAB or MALDI. The TEX results can be useful to analyze the effects of instrumental parameters such as capillary-skimmer voltage in ESI or laser power in MALDI.

Thermal extrapolation analysis is useful especially for energy deposition by dissociative ion–molecule reactions, and for the energetics of activated dissociation of biological and polymer ions. The required Arrhenius parameters are increasing available from ion mobility, TIFT and BIRD measurements.

As for chemical activation, energy deposition by dissociative exothermic charge transfer and proton transfer reactions is of basic interest. Although product distributions are available for thousands of such reactions, energy deposition by these reactions is not well characterized. The available data may be combined with the thermal dissociation parameters of the radical or protonated product ions and thermal extrapolation can then assign the energies deposited in the product ions by these reactions.

In summary, thermal extrapolation yields reasonable ion energies and trends consistent with other energy estimation methods. However, there are only a few systems where chemical or collisional activation data and thermal dissociation parameters are both available. With increasingly available thermal

Table A1
Estimated group frequencies for protonated peptides

	υ (cm^{-1})												
	200	300	400	600	800	1000	1200	1400	1500	1600	1650	3000	3200
N-valeryl leucine[a]	10	10	10	10	10	9	10	10	4	2	2	10	8
LeuEnk[a]	16	16	20	20	20	20	28	28	10	5	5	31	9
Gly5[a]	10	10	10	10	10	9	10	10	4	5	5	10	8
BRAD[a,b]	26	26	34	34	34	34	41	41	23	12	8	49	13

[a] Rows show numbers of oscillators of each frequency group. Frequencies for the non-covalent dimers (Leucine enkephalin)$_2H^+$ and ((Gly)$_5$)$_2H^+$ were derived based on the monomers.

[b] Brad indicates the (des-Arg^9 Bradykinin)$2H^{2+}$ bradykinin analogue.

dissociation data, it will be of interest to compare ion energies obtained from the thermal extrapolation with ion energies estimated by other methods for various fragmentations.

Acknowledgements

We thank Dr. Béla Paizs and Mr. Christian Bleiholder for providing ab inito frequencies of protonated *N*-valeryl leucine and Leucine enkephalin ions. One of us (MM) thanks the National Institute of Standards and Technology for partial funding of this work.

Appendix A

See Table A1.

References

[1] F.H. Field, J. Am. Chem. Soc. 91 (1969) 2827.
[2] F.H. Field, J. Am. Chem. Soc. 91 (1969) 6334.
[3] W.H. Laurie, F.H. Field, J. Am. Chem. Soc. 94 (1972) 2913.
[4] W.H. Laurie, F.H. Field, J. Am. Chem. Soc. 94 (1972) 3359.
[5] M. Meot-Ner (Mautner), F.H. Field, J. Am. Chem. Soc. 95 (1973) 7207.
[6] X. Cheng, Z. Wu, C. Fenselau, J. Am. Chem. Soc. 115 (1993) 4844.
[7] B.A. Cerda, S. Hoyau, G. Ohanessian, C. Wesdemiotis, J. Am. Chem. Soc. 120 (1998) 2437.
[8] P.B. Armentrout, J. Am. Soc. Mass Spectrom. 11 (2000) 371.
[9] S.A. Miller, D.E. Riederer, R.G. Cooks, W.R. Cho, H. Kang, J. Phys. Chem. 98 (1994) 245.
[10] J. Laskin, J.H. Futrell, Mass Spectrom. Rev. 22 (2003) 158.
[11] T. Raz, R.D. Levine, J. Chem. Phys. 105 (1996) 8097.
[12] L. Drahos, K. Vékey, J. Mass Spectrom. 38 (2003) 1025.
[13] L. Drahos, C. Peltz, K. Vékey, J. Mass Spectrom. 39 (2004) 1016.
[14] K.M. Ervin, Int. J. Mass Spectrom. 195–196 (2000) 271.
[15] J. Laskin, J.H. Futrell, Mass Spectrom. Rev. 24 (2005) 135.
[16] P.D. Schnier, J.C. Jurchen, E.R. Williams, J. Phys. Chem. B 103 (1999) 737.
[17] P.R. Kemper, M.T. Bowers, J. Am. Soc. Mass Spectrom. 1 (1990) 197.
[18] M.F. Jarrold, Ann. Rev. Phys. Chem. 51 (2000) 179.
[19] A.I. Fernandez, A.A. Viggiano, A.I. Maergoiz, J. Troe, V.G. Ushakov, Int. J. Mass Spectrom. 241 (2005) 305.
[20] R.C. Dunbar, T.B. McMahon, Science 279 (1998) 194.
[21] R.C. Dunbar, Mass Spectrom. Rev. 23 (2004) 127.
[22] M. Meot-Ner (Mautner), Thermal dissociation of gas phase ions: a review and potential applications, in preparation.
[23] J. Laskin, T.H. Bailey, E.V. Denisov, J.H. Futrell, J. Phys. Chem. A 106 (2002) 9832.
[24] J. Laskin, J.H. Futrell, J. Chem. Phys. 116 (2002) 4302.
[25] J. Laskin, J.H. Futrell, J. Chem. Phys. 119 (2003) 3413.
[26] J.L. Jones, A.R. Dongré, A. Somogyi, V.H. Wysocki, J. Am. Chem. Soc. 116 (1994) 8368.
[27] A.R. Dongré, J.L. Jones, Á. Somogyi, V.H. Wysocki, J. Am. Chem. Soc. 118 (1996) 8365.
[28] G. Tsaprailis, Á. Somogyi, E.N. Nikolaev, V.H. Wysocki, Int. J. Mass Spectrom. Ion Phys. 195/196 (2000) 467.
[29] G. Tsaprailis, H. Nair, Á. Somogyi, V.H. Wysocki, W. Zhong, J.H. Futrell, S.G. Summerfield, S.J. Gaskell, J. Am. Chem. Soc. 121 (1999) 5142.
[30] M. Meot-Ner (Mautner), A.R. Dongré, Á. Somogyi, V.H. Wysocki, Rapid Commun. Mass Spectrom. 9 (1995) 829.
[31] P.D. Schnier, W.D. Price, R.A. Jockusch, E.R. Williams, J. Am. Chem. Soc. 118 (1996) 7178.
[32] P.D. Schnier, W.D. Price, E.F. Strittmatter, E.R. Williams, J. Am. Soc. Mass Spectrom. 8 (1997) 771.
[33] D.J. Butcher, K.G. Asano, D.E. Goeringer, S.A. McLuckey, J. Phys. Chem. A 103 (1999) 8664.
[34] K.G. Asano, D.E. Goeringer, S.A. McLuckey, Int. J. Mass Spectrom. 185–187 (1999) 207.
[35] T. Su, W.J. Chesnavich, J. Chem. Phys. 76 (1982) 5183.
[36] J. Troe, A.A. Viggiano, S. Williams, J. Phys. Chem. A 108 (2004) 1574.
[37] J.H. Moon, J.Y. Oh, M.S. Kim, J. Am. Soc. Mass Spectrom. 17 (2006) 1749.
[38] M.J. Dekrey, H.I. Kenttamaa, V.H. Wysocki, R.G. Cooks, Org. Mass Spectrom. 21 (1986) 193.
[39] R.G. Cooks, T. Ast, A. Mabud, Int. J. Mass Spectrom. Ion Process. 100 (1990) 209.
[40] V.S. Rakov, E.V. Denisov, J.H. Futrell, D.P. Ridge, Int. J. Mass Spectrom. 213 (2002) 25.
[41] V.H. Wysocki, H.I. Kenttamaa, R.G. Cooks, J. Phys. Chem. 92 (1988) 6465.
[42] Z. Herman, J.H. Futrell, B. Friedrich, Int. J. Mass Spectrom. Ion Process. 58 (1984) 181.
[43] R. Worgotter, J. Kubista, J. Zabka, Z. Dolejsek, T.D. Mark, Z. Herman, Int. J. Mass Spectrom. Ion Process. 174 (1998) 53.
[44] J. Zabka, Z. Dlejsek, Z. Herman, J. Phys. Chem. A 106 (2002) 10861.
[45] J. Zabka, Z. Dolejsek, J. Roithova, V. Grill, T.D. Märk, Z. Herman, Int. J. Mass Spectrom. 213 (2002) 145.
[46] Z. Herman, J. Am. Soc. Mass Spectrom. 14 (2003) 1360.
[47] K.Y. Song, O. Meroueh, W.L. Hase, J. Chem. Phys. 118 (2003) 2893.
[48] O. Meroueh, W.L. Hase, Int. J. Mass Spectrom. 201 (2000) 233.
[49] J.P. Wang, S.O. Meroueh, Y.F. Wang, W.L. Hase, Int. J. Mass Spectrom. 230 (2003) 57.
[50] A. Rahaman, J.B. Zhou, W.L. Hase, Int. J. Mass Spectrom. 249–250 (2006) 321.
[51] Y. Wang, W.L. Hase, K.Y. Song, J. Am. Soc. Mass. Spectrom. 14 (2003) 1402.
[52] C. Lifshitz, Int. J. Mass Spectrom. Ion Process. 118 (1992) 315.
[53] L. Drahos, K. Vékey, J. Am. Soc. Mass Spectrom. 10 (1999) 323.
[54] K. Vékey, Á. Somogyi, V.H. Wysocki, J. Mass Spectrom. 30 (1995) 212.
[55] V.S. Rakov, E.V. Denisov, J. Laskin, J.H. Futrell, J. Phys. Chem. A 106 (2002) 2781.
[56] J. Laskin, M. Byrd, J.H. Futrell, Int. J. Mass Spectrom. 195 (2000) 285.
[57] J.N. Louris, R.G. Cooks, J.E.P. Syka, P.E. Kelley, G.C. Stafford, J.F.J. Todd, Anal. Chem. 59 (1987) 1677.
[58] J. Laskin, E. Denisov, J.H. Futrell, J. Am. Chem. Soc. 122 (2000) 9703.
[59] K. Vékey, Á. Somogyi, V.H. Wysocki, Rapid Commun. Mass Spectrom. 10 (1996) 911.
[60] J. Laskin, E. Denisov, J.H. Futrell, J. Phys. Chem. B 105 (2001) 1895.
[61] J. Laskin, J. Phys. Chem. A 110 (2006) 8554.
[62] A.R. Dongré, Á. Somogyi, V.H. Wysocki, J. Mass Spectrom. 31 (1996) 339.